Postfertilization Autophagy of Sperm Organelles Prevents Paternal Mitochondrial DNA Transmission

Sara Al Rawi *et al.*

Science **334**, 1144 (2011);
DOI: 10.1126/science.1211878

Science (print ISSN 0036-8075; online ISSN 1095-9203) is published weekly, except the last week in December, by the American Association for the Advancement of Science, 1200 New York Avenue NW, Washington, DC 20005.

mutant hermaphrodites were mated with wild-type males (Fig. 4B and fig. S7A). Conversely, *lgg-1(tm3489)* mutation in males did not affect clearance of paternal mitochondria in embryos, suggesting that maternally provided autophagic activity is required for effective degradation of sperm-derived mitochondria in the early embryo (fig. S7B). On the other hand, even in embryos from the *lgg-1(tm3489)* hermaphrodites, paternal mitochondria were observed as late as at the lima-bean stage but eventually disappeared at later stages. We assumed that the wild-type *lgg-1* gene provided by the sperm was expressed and may have restored the autophagic activity in late embryos. Supporting this possibility, crossing of *lgg-1(tm3489)* hermaphrodites and wild-type males resulted in viable F1 embryos (fig. S6). To generate *lgg-1(tm3489)* homozygous embryos, MT-labeled *lgg-1(tm3489)* males were crossed with *lgg-1(tm3489)* hermaphrodites. In *lgg-1 (tm3489)* homozygous F1 embryos, MT-labeled paternal mitochondria were detected in late embryos and even in L1 larvae, showing that autophagy is required for elimination of paternal mitochondria (Fig. 4C and fig. S8, A to C). The same results were obtained by using sperm-derived mtGFP (fig. S7, C to F′). In mutant larvae, MT-labeled mitochondria were distributed throughout various tissues. To further detect traces of paternal mtDNA in F1 offspring, we used a large deletion allele of mtDNA (*uaDf5*) (Fig. 4D). In hermaphrodites, *uaDf5* is stably inherited in a heretoplasmic state with the wild-type mtDNA (*24*). When paternal mtDNA was marked with *uaDf5*, it was not normally transmitted to the next generation (Fig. 4E). In contrast, in the *lgg-1(tm3489)* background, paternally provided *uaDf5* was detected in F1 offspring, demonstrating inheritance of paternal mtDNA (Fig. 4F and fig. S8D).

We also examined whether sperm mitochondria were ubiquitinated as reported in mammals (*7*). In sperm, no obvious staining was detected by using an antibody against polyubiquitin (fig. S9A). Instead, punctate structures giving a strong poly-ubiquitination signal appeared around paternal pronuclear DNA in early embryos (fig. S9B). We found that these structures did not directly overlap with paternal mitochondria but colocalized with a marker of membranous organelles (MOs), specialized vesicular structures in sperms (fig. S9D) (*25*). These ubiquitinated MOs were also engulfed by GFP–LGG-1–positive autophagosomes. MOs and paternal mitochondria seemed to be engulfed together or independently by autophagosomes (fig. S9E).

We have shown that autophagy is essential for the effective elimination of paternal mitochondria. Our results also suggest that autophagic degradation of paternal mitochondria could be the mechanism of maternal inheritance of mtDNA. Autophagosomes induced upon fertilization were localized and appeared to selectively engulf sperm components, which is reminiscent of the selective autophagic degradation of damaged mitochondria and invading bacteria in mammals (*26*, *27*). Paternal mitochondria remaining in the *lgg-1* mutant retained the characteristic granular morphology and did not increase in number during embryogenesis (figs. S7 and S8), implying that they are proliferation- and fusion-inactive. Such qualitative difference may underlie selective elimination of paternal mitochondria. The paternal mitochondria and/or mtDNA could be heavily damaged by reactive oxygen species before fertilization (*28*). Selective elimination of paternal mitochondria may prevent the spreading of potentially deleterious mitochondria to the whole population. In mice, autophagy is also up-regulated immediately after fertilization (*12*), suggesting that fertilization-triggered autophagy is a conserved phenomenon in animals.

References and Notes

1. F. Ankel-Simons, J. M. Cummins, *Proc. Natl. Acad. Sci. U.S.A.* **93**, 13859 (1996).
2. K. F. Lindahl, *Trends Genet.* **1**, 135 (1985).
3. U. Gyllensten, D. Wharton, A. Josefsson, A. C. Wilson, *Nature* **352**, 255 (1991).
4. J. M. Cummins, T. Wakayama, R. Yanagimachi, *Zygote* **5**, 301 (1997).
5. H. Kaneda *et al.*, *Proc. Natl. Acad. Sci. U.S.A.* **92**, 4542 (1995).
6. Y. Nishimura *et al.*, *Proc. Natl. Acad. Sci. U.S.A.* **103**, 1382 (2006).
7. P. Sutovsky *et al.*, *Nature* **402**, 371 (1999).
8. N. Mizushima, *Genes Dev.* **21**, 2861 (2007).
9. Z. Xie, D. J. Klionsky, *Nat. Cell Biol.* **9**, 1102 (2007).
10. N. Mizushima, B. Levine, A. M. Cuervo, D. J. Klionsky, *Nature* **451**, 1069 (2008).
11. H. Nakatogawa, K. Suzuki, Y. Kamada, Y. Ohsumi, *Nat. Rev. Mol. Cell Biol.* **10**, 458 (2009).
12. S. Tsukamoto *et al.*, *Science* **321**, 117 (2008).
13. A. Meléndez, B. Levine, *WormBook* **2009**, 1 (2009).
14. Y. Zhang *et al.*, *Cell* **136**, 308 (2009).
15. J. McCarter, B. Bartlett, T. Dang, T. Schedl, *Dev. Biol.* **205**, 111 (1999).
16. D. Greenstein, *WormBook* **2005**, 1 (2005).
17. S. Ward, J. S. Carrel, *Dev. Biol.* **73**, 304 (1979).
18. S. Ward, Y. Argon, G. A. Nelson, *J. Cell Biol.* **91**, 26 (1981).
19. A. Singson, K. B. Mercer, S. W. L'Hernault, *Cell* **93**, 71 (1998).
20. D. P. Hill, D. C. Shakes, S. Ward, S. Strome, *Dev. Biol.* **136**, 154 (1989).
21. W. L. Johnston, A. Krizus, J. W. Dennis, *Curr. Biol.* **20**, 1932 (2010).
22. C. Bucci, P. Thomsen, P. Nicoziani, J. McCarthy, B. van Deurs, *Mol. Biol. Cell* **11**, 467 (2000).
23. M. Sato *et al.*, *EMBO J.* **27**, 1183 (2008).
24. W. Y. Tsang, B. D. Lemire, *Biochem. Cell Biol.* **80**, 645 (2002).
25. S. W. L'Hernault, *WormBook* **2006**, 1 (2006).
26. I. Nakagawa *et al.*, *Science* **306**, 1037 (2004).
27. R. J. Youle, D. P. Narendra, *Nat. Rev. Mol. Cell Biol.* **12**, 9 (2011).
28. R. J. Aitken, *Reprod. Fertil. Dev.* **7**, 659 (1995).

Acknowledgments: We thank K. Sato and other members of Sato's laboratory for technical assistance and discussions; Y. Ohsumi for discussions; S. Mitani, Y. Kohara, and the *Caenorhabditis* Genetic Center for supplying strains and an antibody. This research was supported by a Grant-in-Aid for Young Scientists (A), Japan Society for the Promotion of Science; a Grant-in-Aid for Scientific Research on Priority Areas "Protein Community" and Scientific Research on Innovative Areas "Intracellular Logistics," Ministry of Education, Culture, Sports, Science, and Technology (MEXT); the GCOE Program, MEXT. This research was also supported by the Uehara Memorial Foundation (to K.S.) and the Naito Foundation (to M.S.).

Supporting Online Material

www.sciencemag.org/cgi/content/full/science.1210333/DC1
Materials and Methods
Figs. S1 to S9
Table S1
References (*29*–*39*)

27 June 2011; accepted 22 September 2011
Published online 13 October 2011;
10.1126/science.1210333

Postfertilization Autophagy of Sperm Organelles Prevents Paternal Mitochondrial DNA Transmission

Sara Al Rawi,[1,2] Sophie Louvet-Vallée,[1,2] Abderazak Djeddi,[1,2] Martin Sachse,[3] Emmanuel Culetto,[4] Connie Hajjar,[5] Lynn Boyd,[5] Renaud Legouis,[4]* Vincent Galy[1,2]*†

In sexual reproduction of most animals, the spermatozoon provides DNA and centrioles, together with some cytoplasm and organelles, to the oocyte that is being fertilized. Paternal mitochondria and their genomes are generally eliminated in the embryo by an unknown degradation mechanism. We show that, upon fertilization, a *Caenorhabditis elegans* spermatozoon triggers the recruitment of autophagosomes within minutes and subsequent paternal mitochondria degradation. Whereas the nematode-specific sperm membranous organelles are ubiquitinated before autophagosome formation, the mitochondria are not. The degradation of both paternal structures and mitochondrial DNA requires an LC3-dependent autophagy. Analysis of fertilized mouse embryos shows the localization of autophagy markers, which suggests that this autophagy event is evolutionarily conserved to prevent both the transmission of paternal mitochondrial DNA to the offspring and the establishment of heteroplasmy.

In most metazoans the mitochondrial DNA (mtDNA) is maternally inherited (*1*), and typically, individuals harbor a unique mtDNA genotype defining the homoplasmic state. Heteroplasmy, the occurrence of more than one mtDNA genotype, is rare and results from spontaneous

modifications of maternal mtDNA or paternal contribution upon fertilization (*2*). In mice and *C. elegans*, heteroplasmy can be inherited through the female germ line but not through spermatozoa (*3*, *4*). Paternal mitochondria and their mtDNA are eliminated, but the mechanism is not yet understood. Studies in mammals have suggested that elimination of paternal mitochondria is dependent on a mechanism involving ubiquitination and the lysosomal pathway (*5*). Furthermore, medaka sperm mtDNA appears to be progressively degraded 30 to 60 min after fertilization by an unknown mechanism (*6*).

Autophagy is a major ubiquitous catabolic process in eukaryotes allowing the degradation of cytoplasmic constituents and organelles by selective or nonselective sequestration in double-membrane vesicles, the autophagosomes (*7*). In the mouse early embryo, autophagy is essential for preimplantation development (*8*) and has been postulated to degrade maternal proteins. However, its role in the elimination of paternal inherited components remains elusive. To address this question, we analyze the fate of sperm components in the *C. elegans* embryo (Fig. 1A) (see also supporting online materials and methods). Here, we show that upon fertilization, several sperm components, including mitochondria, enter the oocyte and are rapidly degraded by autophagy.

C. elegans mature spermatozoa contains membranous organelles (MOs) that represent nematode-specific membrane compartments and are present either underneath or fused with the plasma membrane (Fig. 1A) (*9*). Their function is unclear, but MO fusion is essential for sperm motility (*10*). *C. elegans* spermatozoa also contain mitochondria and high amounts of the major sperm proteins (MSPs) concentrated in the pseudopod and required for sperm motility (Fig. 1A). To analyze which of these components enter the oocyte upon fertilization, we used antibodies specific for the MOs or the MSPs and the inner mitochondrial membrane adenine nucleotide transporter ANT-1.1 fused to green fluorescent protein (GFP) (*11*) or CMXRos mitotracker to label mitochondria. After crossing labeled males with wild-type (WT) hermaphrodites, we analyzed the presence of MOs, MSPs, mitochondria, and sperm nuclear DNA in the progeny (Fig. 1 and fig. S2, A and B). After fertilization, both MOs and sperm mitochondria enter and remain close to the sperm DNA at the posterior pole of the embryo (Fig. 1, C and D). MSPs are uniformly distributed in newly fertilized embryos up to the two-cell stage (fig. S2A) with no enrichment around sperm DNA (fig. S2B).

To test whether sperm entry could trigger an autophagic response, we stained embryos using antibodies for *C. elegans* Atg8/LC3 ubiquitin-like proteins: LGG-1 and LGG-2 (*12*). Both are recruited to the membrane of the autophagosomes and are good markers for macroautophagy (*13*). At 15 to 30 min postfertilization, prominent LGG-1– and LGG-2–positive structures appear next to the sperm DNA (Fig. 1, C, D, and F). Controls demonstrate that this staining is specific (fig. S1, E to H) and is absent in the mature spermatozoa (Fig. 1B). Time-lapse analysis using a GFP::LGG-2 revealed that these large structures are dynamic, tend to cluster around the sperm DNA, then segregate during the first mitotic divisions close to the cortex (movie S1) and disappear. LGG-1/LGG-2 signal surrounds MOs and paternal mitochondria, suggesting that these organelles are enwrapped by autophagosomes (Fig. 1, C, D, and F). This sperm-specific recruitment was confirmed in polyspermic *egg-4/5(RNAi)* embryos (RNAi, RNA interference) (*14*) in which LGG-2 autophagic structures are associated with MOs around each sperm DNA (fig. S1I). Electron microscopy analyses showed that after fertilization, mitochondria are found in double-membrane vesicles (Fig. 1E) in the cortical region,

[1]Université Pierre et Marie Curie–Paris VI, UMR7622–Biologie du Développement, 9 Quai St. Bernard, 75005 Paris, France. [2]CNRS, UMR7622–Biologie du Développement, 9 Quai St. Bernard, 75005 Paris, France. [3]Plateforme de Microscopie Ultrastructurale, Imagopole, Institut Pasteur, 25 rue du Docteur Roux, 75015 Paris, France. 4Centre de Génétique Moléculaire–UPR3404–CNRS–Université Paris XI, Avenue de la Terrasse, 91198 Gif Sur Yvette, France. [5]Department of Biological Sciences, University of Alabama, Huntsville, Huntsville, AL 35899, USA.

*These authors contributed equally to this work.
†To whom correspondence should be addressed. E-mail: vgaly@snv.jussieu.fr

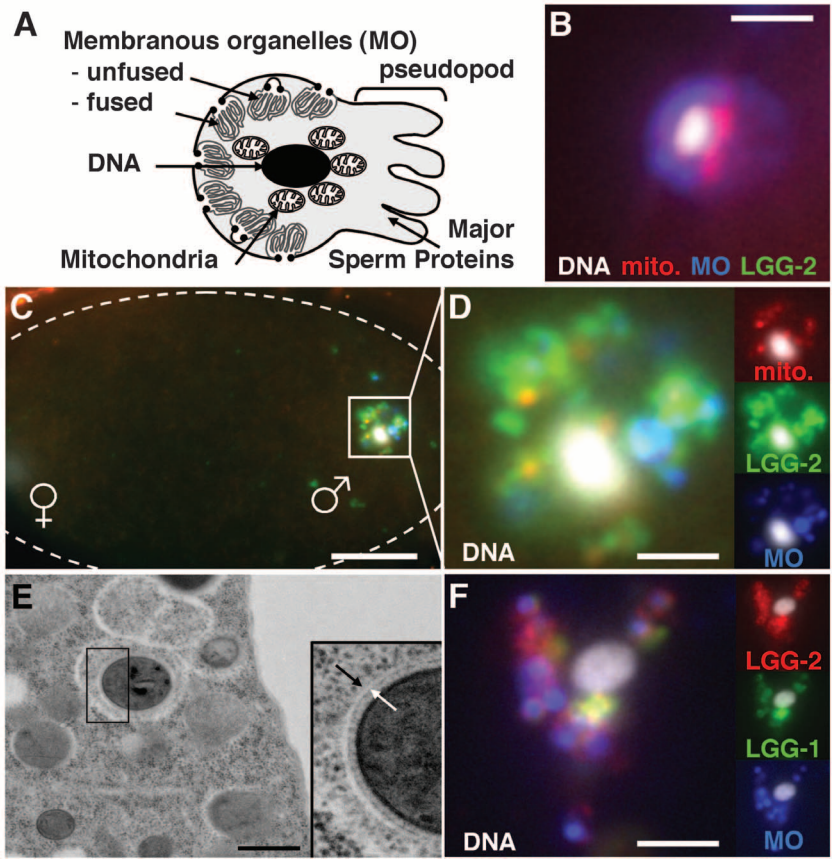

Fig. 1. The entry of spermatozoon organelles in the *C. elegans* oocyte at fertilization induces autophagy. (**A**) Schematic representation of a *C. elegans* spermatozoon. (**B** to **D**) Spermatozoon is devoid of LGG-2 (green) but transmits MOs (blue), CMXRos-labeled mitochondria (red), and DNA (white) (B) to the oocyte upon fertilization (C). (D) Magnified view of the sperm DNA (white) region. Twenty min after fertilization, organelles are associated with LGG-2 (green)–positive structures. Insets correspond to the split channels. (**E**) Transmission electron microscopy image of the cortical area of a two-cell-stage embryo revealing the presence of autophagosomes around mitochondria. Arrows indicate the limiting double membrane. (**F**) The two LC3 homologs, LGG-2 (red) and LGG-1 (green), are recruited to the MOs (blue) around sperm DNA (white). Scale bars: 2 μm in (B), (D), and (F); 10 μm in (C); 500 nm in (E). The dotted lines in (C) indicate the border of the embryo; male (♂) and female (♀) DNA are indicated.

demonstrating that mitophagy does occur at that time.

In mammals, ubiquitination of sperm mitochondria has been proposed to be the signal for their degradation (*5*). To test whether ubiquitination could serve as a mark for autophagy degradation in spermatozoa and early embryos, we used an antibody specific for ubiquitin conjugates in combination with either CMXRos-labeled sperm mitochondria or MO antibody (Fig. 2). We found that the ubiquitin antibody stains MOs, but not mitochondria, in mature spermatozoa and in newly fertilized embryos (Fig. 2, A to D). Using GFP::ubiquitin expressing worms, we observed its recruitment on structures around sperm DNA within 3 min after fertilization, suggesting that sperm components are further ubiquitinated after they enter the oocyte (Fig. 2E and movie S2), and confirmed that sperm-inherited mitochondria are not ubiquitinated (fig. S3). Several types of ubiquitin modification exist, depending on the number and the branching of the ubiquitin moiety. Ubiquitin chains linked via their lysine-48 residue (K48-linked) can target the substrate for proteasome degradation, whereas K63-linked chains are associated with the autophagic pathway (*15*). Costaining MOs and mitochondria with either K63- or K48-specific antibodies (Fig. 2F) reveals that MOs are decorated only in the embryo with both K63 and K48 ubiquitin chain antibodies. K63 ubiquitination of MOs precedes LGG-1/2 recruitment and autophagosome formation and is likely to be the signal for autophagy of these sperm organelles. The presence of the K48-linked chains signal and the 19*S* regulatory subunit of the proteasome around MOs (Fig. 2F) suggests that some proteasome activity could also be involved in MO degradation. But unlike the autophagy markers, the 19*S* subunit is inherited from the spermatozoa (Fig. 2F), suggesting a role before fertilization. Together, these data demonstrate that after fertilization, both MOs and mitochondria are associated with autophagosomal structures, although only MOs are ubiquitinated.

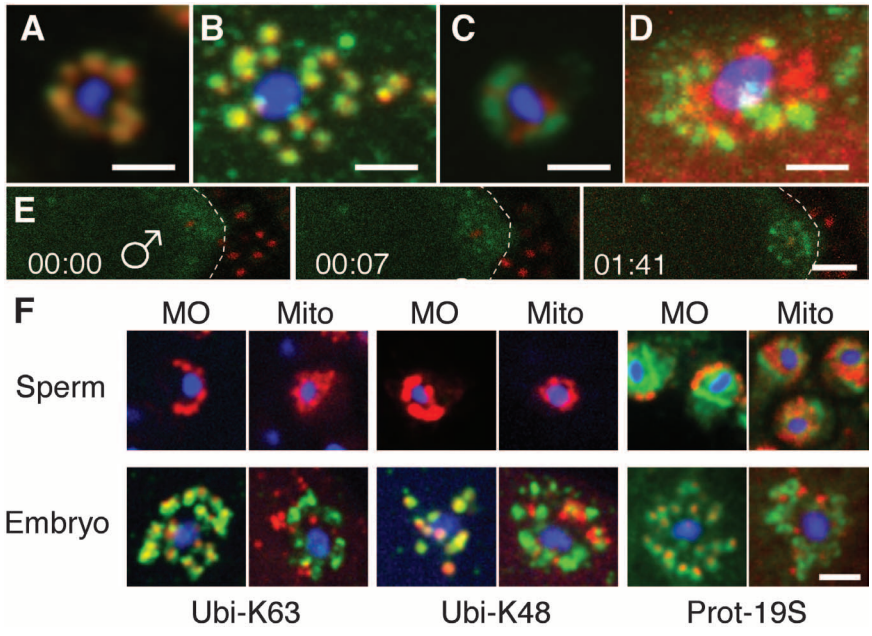

Fig. 2. Paternal inherited MOs are rapidly K63 and K48 ubiquitinated after fertilization, but mitochondria are not ubiquitinated. (**A** to **D**) MOs [red in (A and B)], but not mitochondria [red in (C and D)], are ubiquitinated (green) in the spermatozoon (A and C) and around sperm DNA after fertilization (B and D). (**E**) Still images of a confocal movie showing GFP::ubiquitin (green) recruitment around sperm chromatin (mCherry Histone-H2B, red) after fertilization, time indicated in minutes:seconds. (**F**) MOs (red) in the sperm DNA (blue) region are positive for K63 and K48 ubiquitination (green) but negative before fertilization. Mitochondria (red) remain negative (movie S3). The proteasome 19*S* subunit (green) is found in the spermatozoa, then around MOs but not mitochondria (red) after their entry. Scale bars: 2 μm in (A) to (D) and (F); 5 μm in (E).

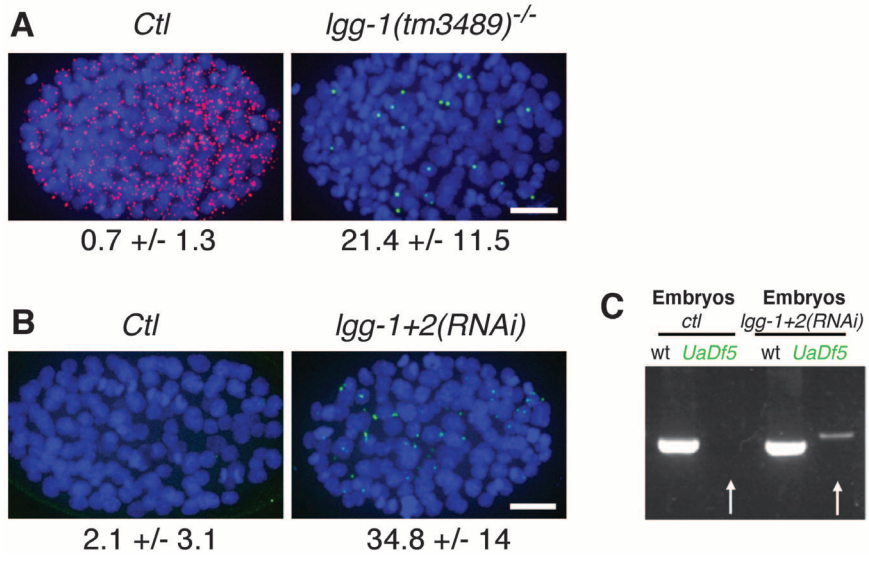

Fig. 3. Autophagy is required to degrade *C. elegans* spermatozoon inherited organelles after fertilization and prevent mitochondrial heteroplasmy. (**A**) Z-projections of confocal stacks. MOs (green) are absent in WT (Ctl) but remain in *lgg-1(tm3489)* 120-cell embryos. LGG-1 (red) is absent in the mutant embryo. Average number and SD of the remaining MO structures in 100/120-cell stage control (n = 22) and *lgg-1(tm3489)* (n = 10) embryos are indicated. (**B** and **C**) Paternal mitochondria and their DNA persist in autophagy-defective embryos. (B) Paternal mitochondria visualized by CMXRos mitotracker (green) are absent at the 100/120-cell stage in controls (n = 31), whereas they persist in *lgg-1+2(RNAi)* (n = 23) embryos. Average numbers of the remaining CMXRos and SDs are indicated below. Scale bars: 10 μm. (C) Interfering with autophagy maintains paternal mitochondrial heteroplasmy. Heteroplasmic males carrying both deleted (*UaDf5*) and WT mtDNA were crossed with control or *lgg-1+2(RNAi)* hermaphrodites, and their embryos progeny were tested by PCR for the presence of WT and *UaDf5* mtDNA. Male *UaDf5* mtDNA is detected in autophagy-deficient embryos, but not in control, indicating a heteroplasmic state.

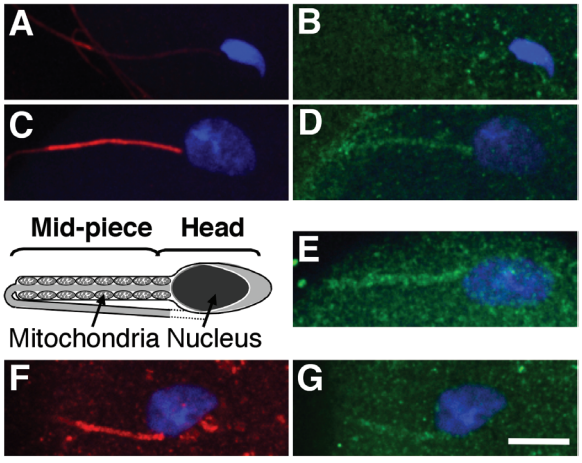

Fig. 4. Fertilization of the mouse oocyte induces recruitment of autophagy markers around the flagellum midpiece of the spermatozoon. The scheme represents the morphology of mouse spermatozoon with only a part of the flagellum. (**A** and **C**) Maximum intensity projection of Z-stacks of confocal images of the entire volume of the oocyte or of three consecutive images (**E**) or single confocal images (**B**, **D**, **F**, and **G**). (A and B) Unfertilized or (C to G) fertilized mouse oocytes stained for sperm DNA (blue), immmunostained for ubiquitin (red) (A and C), LC3 (green) (B and D), GABARAP (green) (E), and K63-linked ubiquitin (F) together with P62 (G). The staining appears in the midpiece associated with the partially decondensed male pronucleus (C to G), whereas only faint (A) or no (B) signals are visible in the midpiece of external spermatozoa (A and B). Scale bar: 5 μm.

To confirm that the formation of autophagic structures is involved in the degradation of sperm organelles, we used *lgg-1(tm3489)* mutant and *lgg-1+2(RNAi)* to inactivate autophagosome formation in the oocyte. In control embryos the number of MOs rapidly decreases during the first cell divisions, whereas in mutant and RNAi embryos, MOs are still present at 100/120-cell stage (Fig. 3A and fig. S4A). To confirm that the persistence of MOs is due to the reduction of the autophagy activity we depleted two other proteins involved in autophagic pathway: ATG-7, the E1-like activating enzyme required for ATG8/LC3/LGG-1 activation (*16*), and the small guanosine triphosphatase Rab7 involved in the fusion of autophagosomes with lysosomes (*17*). Both depletions induce an alteration of LGG-2 signal and a persistence of MOs (fig. S2, C and D) supporting the notion that MOs are degraded by macro-autophagy.

We then analyzed whether paternal mitochondria, which are not ubiquitinated but are closely associated with LGG-1/LGG-2 autophagic structures in the one-cell embryo, are also degraded by autophagy. We crossed ANT-1.1::GFP– and CMXRos-labeled males with control and *lgg-1+2(RNAi)* hermaphrodites, and we analyzed the presence of paternal mitochondria in their progeny. Whereas in control embryos paternal mitochondria are not detected from the 8/10-cell stage, they are maintained in *lgg-1+2(RNAi)* embryos (Fig. 3B and fig. S4B). The persistence of paternal mitochondria in defective autophagy conditions suggests that paternal mtDNA could also persist in embryo. To track paternal mtDNA in the fertilized embryos, we used males from the LB138 strain, which contains both WT and deleted mtDNA (*UaDf5*) (*4*). When LB138 males were crossed with control worms, we were not able to amplify the paternal mtDNA in the progeny by polymerase chain reaction (PCR) (Fig. 3C and fig. S4C), confirming that it is efficiently degraded in WT embryos. However, in *lgg-1+2 (RNAi)* embryos, the paternally inherited mitochondrial DNA was detected in 2- to 6-hour-old embryos (80 to 500 cells) (Fig. 3C). Taken together, these data indicate that after fertilization, paternal mitochondria and their genomes are quickly degraded by autophagy and that inactivation of autophagy results in heteroplasmy in the embryo.

Our findings in *C. elegans* demonstrate that spermatozoon fertilization of the oocyte triggers a selective autophagic process that recognizes and degrades paternally inherited organelles but not cytoplasmic MSPs. In mammals, ubiquitinated sperm mitochondria, localized in the midpiece of the flagellum, enter the oocyte after gamete fusion and are degraded by an unknown mechanism (*5*). Mouse oocyte fertilization induces two essential waves of autophagy several hours after sperm entry that have been hypothesized to participate in the degradation of maternal material (*9*). To test whether autophagy of spermatozoon components could be conserved in mammals, we costained fertilized mouse oocytes with anti-ubiquitin and anti-LC3 antibodies. As reported (*5*), ubiquitinated mitochondria are detected in the midpiece of the sperm before [21 ubiquitinated mitochondria out of 21 spermatozoa before fertilization (21/21)] and, even brighter, after fertilization (23/24) (Fig. 4, A and C, and fig. S5, A, B, E, and F). We observed that the midpiece was stained with the LC3 antibody after fertilization (13/13) and not in spermatozoa outside the oocyte (3/3) (Fig. 4, B and D, and fig. S5, C, D, G, and H). We further confirmed that autophagy hallmarks label the mid-piece of spermatozoa using antibodies against gamma-aminobutyric acid receptor–associated protein (GABARAP), another ATG8 homolog (9/9), and Ubi-K63 and P62 (42/49), an autophagic adaptor (Fig. 4, E, F, and G, and fig. S5, I and J; K, L, O, and P; M, N, Q, and R, respectively). Recruitment of autophagosomal markers in the vicinity of ubiquitinated mitochondria suggests that this autophagy could also exist in mammals and be involved in the degradation of sperm-inherited mitochondria. It is notable that, in *C. elegans*, the paternal mitochondria are not ubiquitinated, which indicates that this autophagy is able to degrade both ubiquitinated and nonubiquitinated substrates. It is possible that the mitochondria are incorporated into autophagosomes due to their close association with ubiquitinated MOs. Deciphering the signaling cascade that triggers spermatozoon autophagy and the mechanisms underlying the selectivity of this response would help us to better understand this process and could affect human medically assisted reproduction or animal cloning.

References and Notes

1. C. W. Birky Jr., *Annu. Rev. Genet.* **35**, 125 (2001).
2. M. Schwartz, J. Vissing, *N. Engl. J. Med.* **347**, 576 (2002).
3. B. J. Battersby, J. C. Loredo-Osti, E. A. Shoubridge, *Nat. Genet.* **33**, 183 (2003).
4. W. Y. Tsang, B. D. Lemire, *Biochem. Cell Biol.* **80**, 645 (2002).
5. P. Sutovsky *et al.*, *Nature* **402**, 371 (1999).
6. Y. Nishimura *et al.*, *Proc. Natl. Acad. Sci. U.S.A.* **103**, 1382 (2006).
7. T. Yoshimori, T. Noda, *Curr. Opin. Cell Biol.* **20**, 401 (2008).
8. S. Tsukamoto *et al.*, *Science* **321**, 117 (2008).
9. N. L. Washington, S. Ward, *J. Cell Sci.* **119**, 2552 (2006).
10. S. Ward, Y. Argon, G. A. Nelson, *J. Cell Biol.* **91**, 26 (1981).
11. F. Farina *et al.*, *Dev. Dyn.* **237**, 1668 (2008).
12. Y. Tian *et al.*, *Cell* **141**, 1042 (2010).
13. A. Alberti, X. Michelet, A. Djeddi, R. Legouis, *Autophagy* **6**, 622 (2010).
14. J. M. Parry *et al.*, *Curr. Biol.* **19**, 1752 (2009).
15. V. Kirkin, D. G. McEwan, I. Novak, I. Dikic, *Mol. Cell* **34**, 259 (2009).
16. C. Kang, Y. J. You, L. Avery, *Genes Dev.* **21**, 2161 (2007).
17. S. Jäger *et al.*, *J. Cell Sci.* **117**, 4837 (2004).

Acknowledgments: We thank C. Pappatico, T. Le, and C. Lefebvre for valuable technical assistance during all stages of this project; the staff of the IFR83 Imaging Platform for their efficient help with confocal imaging; K. Wassmann for providing access to research equipments; L. Kuras for advice for quantitative PCR; H. Zhang, S. Strome, and T. Ueno for sharing reagents; J. Plastino for generously providing unpublished reagents for MSP analysis; and A. Golden for assistance with the GFP::ubiquitin project. We also wish to thank P. Codogno and V.G.'s and R.L.'s lab members for careful reading of the manuscript. The LB138 strain was provided by the *Caenorhabditis* Genetics Center, which is funded by the NIH National Center for Research Resources. This research was supported by the NIH (grant GM065444-03 to L.B.), the Centre National de la Recherche Scientifique (R.L. and Action Thématique Incitative sur Programme grant to V.G.), the Univ. of Pierre and Marie Curie, the Agence Nationale de la Recherche (grant ANR 07-BLAN-0063-21 to V.G.), and the Association pour la Recherche contre le Cancer (R.L.).

Supporting Online Material

www.sciencemag.org/cgi/content/full/science.1211878/DC1
Materials and Methods
Figs. S1 to S5
References
Movies S1 to S3

29 July 2011; accepted 11 October 2011
Published online 27 October 2011;
10.1126/science.1211878

Supporting Online Material for

Postfertilization Autophagy of Sperm Organelles Prevents Paternal Mitochondrial DNA Transmission

Sara Al Rawi, Sophie Louvet-Vallée, Abderazak Djeddi, Martin Sachse, Emmanuel Culetto, Connie Hajjar, Lynn Boyd, Renaud Legouis, Vincent Galy*

*To whom correspondence should be addressed. E-mail: vgaly@snv.jussieu.fr

Published 20 October 2011 on *Science* Express
DOI: 10.1126/science.1211878

This PDF file includes

Other Supporting Online Material for this manuscript includes the following:
(available at www.sciencemag.org/cgi/content/full/science.1211878/DC1)

Materials and Methods

C. elegans genetics and RNAi

Nematode strains were grown on NGM plates seeded with *E. coli* strain OP50 and handled as described *(S1)*. The wild type parent strain used was the *C. elegans* N2 Bristol variety. Transgenic strains VIG06 [*gfp::lgg-2; unc-119(+)*], and VIG03 [*ant-1.1::GFP; unc-119(+)*] were obtained by biolistic transformation *(S2)* using previously described constructs *(11, 13)* and screened for expression in the germline. The strain LN130 [*pie-1p::GFP::ubiquitin + unc-119(+); pie-1p::mCherry::his-58*] was obtained by biolistic transformation of the ubiquitin construct and then crossing in the mCherry::histone transgene (*itIs37*). The *lgg-1(tm3489)* mutant was previously described *(13)*. The strain LB138 [*him-8(e1489)IV; uaDf5/+*] is heteroplasmic for its mtDNA (WT and uaDf5 deleted mtDNA molecules coexist) *(4)* and was obtained from the Caenorhabditis Genetics Center.

Bacterial clones from the J. Ahringer library (*rab-7*, *atg-7* and *egg-4/5* and empty vector L4440 for control) were used for RNAi "feeding" experiments *(S3)*. *Lgg-1+2* RNAi experiments were performed by micro-injection. dsRNA for *lgg-1* and *lgg-2* were synthesized with the Maxiscript kit (Ambion) from PCR products containing T7 promoter sequences and then mixed in equal amount before injection in L4 hermaphrodites worms. Uninjected animals from the same population were used as control. After recovering over night, hermaphrodites were transferred to a new plate and when necessary crossed with males. Every 12 hours, animals were transferred to new plates and their progeny recovered for analysis. Efficiency of RNAi was controlled by verifying that 100% of the *lgg-1+2 (RNAi)* progeny die as late embryos or L1 larvae. Efficiency of the crosses was checked in control crosses where 50% of the progeny were males and by genotyping the hermaphrodites for the presence of male mtDNA.

mtDNA genotyping

PCR amplifications of wild-type and the 3.1 kb deleted *Uadf5* mtDNA were performed with specific pairs of primers, which amplify a 925pb and a 1040pb product, respectively. To avoid contamination by sperm from males, hemaphrodites alone where transferred to fresh plates twice and then allowed to laid eggs for 1 to 4 hours period. 20 to 50 animals were collected and lysed for 60 minutes at 65°C in 10 to 30µl of buffer (50mM KCl, 10mM Tris, 20mM MgCl2, 0.45% NP40, 0.45% Tween-20, 0.01% gelatin) containing 1mg/ml proteinase K. Embryos were quickly washed on the plate then collected in the tube cap and squashed using a coverslip piece to break the egg shell prior to lysis. 3µl of lysed animals were used for 35 cycles PCR using DreamTaq polymerase and buffer (Fermentas), then analysed on agarose gel. Results were then confirmed and quantify by real time PCR using Lightcycler 480 with Takara buffer. The sequences of all primers can be obtained upon request.

Production of antibodies against LGG-2

Polyclonal antibodies were obtained after immunization of rabbits and affinity purification with a mixture of two synthetic peptides corresponding to amino-acids 14-27 and 97-114 of *C. elegan* LGG-2 protein (CE06627, Wormbase release WS225).

Immunofluorescence

C. elegans embryo immunostainings were performed as previously described *(S4)* using rabbit polyclonal anti-LGG-2 (1:200), rat polyclonal anti-LGG-1 (1:1000, *(12)*), mouse monoclonal anti-membranous organelles SP56 antibody (1:500, *(10)*) andrabbit polyclonal anti-MSP (1:100) that was generously provided by J. Plastino. Ubiquitinated conjugates were detected

using an affinity purified rabbit polyclonal anti-ubiquitin (Z0458, 1:50, Dako); assessment of ubiquitin chain specificity was performed using either K63 (Apu3, 1:200, Millipore) or K48 (Apu2, 1:600, Millipore) ubiquitin purified rabbit monoclonal antibodies *(S5)*. The 19S regulatory subunit of the proteasome was localized using a rabbit polyclonal antibody (Ab2942, 1: 300, Abcam).

Mouse embryos were recovered as previously described *(S6)*. Briefly, 9 to 12 weeks old females OF1 (Charles River) were super-ovulated by intra-peritoneal injection of 5 UI Pregnant Mare Serum gonadotrophin (PMS, Intervet) and 5 UI human Chorionic Gonadotrophin (hCG, Intervet), 48 hours later. Females were mated with OF1 males (fertilization occurs about 12 hours post-hCG). Early one-cell stage embryos were collected in M2+BSA (4mg/ml) medium at 15 hours post-hCG in oviducts ampullæ's. The cumulus cells were dispersed by incubation in 0,1M hyaluronidase (Sigma). Immunostaining was done after 10 minutes of cold methanol fixation and stained using rabbit polyclonal antibodies against human GABARAP (1:50, gift from T. Ueno), monoclonal antibody against Human LC3 (1:50, gift from T. Ueno), affinity purified rabbit polyclonal anti-ubiquitin (Z0458, 1:50, Dako), affinity purified monoclonal anti K63-linked ubiquitin (Apu3, 1:200, Millipore) and mouse monoclonal antibodies against p62/SQSTM1 (2C11, 1:200, Abnova).

For fluorescent secondary antibodies we used anti-mouse Alexa-488, anti-mouse Alexa-633, anti-rat Alexa-568, anti-rabbit Alexa-633 (1:800, Molecular Probes), anti-rabbit Alexa-488 (1:800, Invitrogen), anti-rabbit and anti-mouse-Cy3 (1:400, Jackson ImmunoResearch Laboratories), and anti-human FITC (1:50, Zymed Laboratories). DNA was stained using Hoechst 33342 (1ug/ml, Fluka analytical, Sigma-Aldrich).

Light microscopy imaging

Immunofluorescence images were collected using a 63X or 100X objective either on an inverted DMI 4000 microscope (Leica) equipped with a Coolsnap fx (Photometrix) digital camera controlled by micromanager software (Fig1B-D, F; S1A-I; S2A, B, D and S4B), on a SP5 confocal scanning microscope (Leica) (Fig2A-E; S3A,B and Movie S7) or a Spinning Disk Confocal microscope (Roper Scientific) equipped with a QuantEM (Photometrix) EMCCD camera controlled by Metamorph software (FigS2C and S4A). Live recording of the *C. elegans* embryos expressing GFP::LGG-2 was done on a Spinning Disk Confocal microscope (Roper Scientific) equipped with a Evolve (Photometrix) EMCCD camera controlled by Metamorph software (Movie S6) as well as immunofluorescence images (Fig2F; 3A, B; 4; S3C-K; S5 and Movie S8).

Mitochondria staining using Mitotracker

The mitochondria of *C. elegans* were stained using Mitotracker Red CMXRos (Molecular Probes), a red fluorescent dye, which stains mitochondria in live cells. Males were grown overnight in the dark at 20°C on NGM plates supplemented with 1µg/ml of CMXRos *(13)* before being used in the crosses.

Transmission electron microscopy

Young worms were frozen in M9 buffer with 20% BSA in a brass planchette, Type A (Agar Scientific). With the flat side of the complementary Type B planchette the filled planchette was closed and frozen with the HPM 010 (BalTec, now Abra Fluid AG). Freeze substitution was

performed in anhydrous acetone containing 2% OSO4 + 0.25% uranylacetate + 2% H2O + 2.5% MeOH (Merck) in a freeze substitution device (Leica). Afterwards samples were embedded stepwise in Epon. After polymerization thins sections were cut with a Ultracut UCT microtome (Leica). Sections were collected on 50 mesh formvar coated cupper grids and poststained with 4% uranylacetate and Reynold's lead citrate. Images were taken with a Jeol 1010 at 80 kV and equipped with a keen view camera (Soft imaging systems).

Fig. S1.

(A, B) GFP::LGG-2 (green) is recruited around sperm DNA (blue) and immunostained membranous organelles (red) at the posterior pole of the newly fertilized embryo. **(B)** magnified view and split channels of the sperm DNA area. **(C)** Paternal mitochondria positive for ANT-1.1::GFP (green) enter the embryo and are associated with immunostained LGG-2 positive structures (red) around sperm DNA (blue) at the time of meiosis II (20 min post fertilization). **(D)** Magnified view and split channels of the sperm DNA area. **(E-H)** Anti-LGG2 antibody (green) specifically stains structures close and around MO (red) in the 1-cell stage control embryo **(E, F)** but this staining is absent in the *lgg-1+2(RNAi)* embryo **(G, H)**. **(F, H)** Magnified view of the sperm DNA (blue) region, 20 minutes after fertilization, LGG-2 (green) is present **(F)** or absent **(H)** around MO (red). **(I)** Polyspermic embryo with two spermatozoa DNA, each associated with MO (red) and LGG-2 positive autophagic structures (green). Scale bars are 10 µm except 2µm in B and D.

Fig. S2.

(A, B) Major Sperm Protein (MSP) which is very abundant in sperm (arrow in A) where it forms thin filaments *(S7)*, enters the embryo upon fertilization, but does not reveal enrichment around sperm DNA and is degraded at the 2 to 4-cell stage transition. **(A)** Low magnification view of the germline of a WT hermaphrodite worm stained with anti MSP antibody (arrowhead indicates the spermatheca) and magnified view of a 2 and 4 cell stage embryos (inset). **(B)** After fertilization, MSP (green) is evenly distributed trough the entire cytoplasm of the embryo with no enrichment in the sperm DNA area (inset). **(C)** Interfering with autophagy by depleting ATG-7 reduces the amount of LGG-2 positive structures and prevents MO degradation. LGG-2 membrane associated

signal is largely reduced upon ATG-7 depletion (second row, left panel and red in the merge) and MOs (middle panel and green in the merge) persist in *atg-7(RNAi)* embryo (second row) while they are absent in control embryo (first row) of the same stage. **(D)** Interfering with autophagosome/lysosome fusion by depleting RAB-7 increases LGG-2 signal and prevent MO degradation. LGG-2 membrane associated signal is increased upon RAB-7 depletion (second row, left panel and red in the merge) and MO (middle panel and green in the merge) persist in *rab-7(RNAi)* depleted embryo (second row) while they are absent in a control embryo (first row) of the same stage. Scale bars are 10 µm.

Fig. S3. Related to figure 2

(A, B) Sperm inherited mitochondria are not ubiquitinated. Overview of an embryo surrounded by spermatozoa. CMXRos labeled mitochondria (red) inherited from a spermatozoon are visible on the posterior side of the fertilized embryo. These paternal mitochondria do not colocalize with the GFP::ubiquitin positive structures (green). **(B)** Magnified view of the sperm DNA area. Scale bar is 10 µm. **(C-H)** Mitochondria (red) are not K63 (green in D, E) or K48 ubiquitinated (green in **G, H**) neither in the spermatozoon **(C, F)** nor around sperm DNA after fertilization **(D, E, G, H)**. **(I-K)** The proteasome 19S subunit (green) and the paternal mitochondria do not colocalize in sperm **(I)** or after fertilization **(J, K)**. D, G, J are overviews of embryos and E, H, K are magnified views of the sperm DNA area. Scale bar are 2 µm or 10 µm for A, D, G, J.

Fig. S4. Related to figure 3

(A) In 120-cell embryo the MO (green) are absent in control (left) but remain in *lgg-1+2(RNAi)* embryo (arrowheads in right panel). Pictures are Z-projections of confocal stacks. Mean and standard deviation of the remaining MO structures in control (n=21) and *lgg-1+2(RNAi)* (n=6) embryos are indicated below. **(B)** Paternal mitochondria persist in autophagy defective embryos. Paternal mitochondria visualized by ANT-1.1::GFP (green) are visible around sperm DNA (blue) after fertilization (upper panels) but are absent at the 12-cell stage in control while they persist in *lgg-1+2(RNAi)* embryo (arrowheads in lower panels). Scale bars are 10 µm. **(C)** Schematic representation of the crosses and control PCR for the figure 3D. Heteroplasmic males carrying both deleted (*UaDf5*, green) and WT (grey) mtDNA were crossed with either control or *lgg-1+2(RNAi)* hermaphrodites and their embryos progeny were tested by PCR for the presence of WT (WT) and mutated (*UaDf5*) mtDNA. Presence of male UaDf5 mtDNA in hermaphodites after crosses is due to the presence of sperm in their spermatheca and validates the efficiency of the cross. Paternal mtDNA is detected in autophagy deficient embryos, but not in control (arrows).

Fig. S5. Related to figure 4

The entry of spermatozoon organelles in the mouse oocyte at fertilization induces recruitment of autophagy markers around the flagellum mid-piece. Maximum intensity projection of Z-stacks of confocal images of the entire volume of the oocyte **(A, B, E, F)** or of 3 consecutive images (**J, K)** or single confocal images **(C, D, G, H)**. Unfertilized **(A-D)** or fertilized **(E-R)** mouse oocytes stained for DNA (blue) of polar body (Pb), Sperm (Sp) and (♂) or female (♀) pronuclei, immmunostained for ubiquitin (red) **(A, B, E, F)**, LC3 (green) **(C, D, G, H)** and GABARAP (green) **(I, J)**. K63-linked ubiquitin **(K, L, O, P)**, P62 **(M, N, Q, R)** staining appears in the mid-

piece associated with the partially decondensed male pronucleus while no ubiquitin **(A)** nor LC3 **(B)** signal is visible in the mid-piece of external spermatozoa (Sp). P62 and K63-linked ubiquitin staining increases while pronuclei DNA decondenses (compare K-N to O-R). Scale bars are 20 µm in A, C, E, G, I, K, M, O, Q, and 5 µm in B, D, F, H, J, L, N, P, R.

Movie S1

GFP::LGG-2 is recruited around sperm DNA after oocyte fertilization and forms highly mobile structures. Embryo was observed on a Spinning Disk microscope. Every 30 seconds a single transmission image as well as a Z-stack of 10 images every 1.5 µm for the GFP channel were recorded. The movie combines the transmission images (bottom) and the maximum intensity projection of the GFP images (top) for each time-point. Posterior pole is on the right. Playback: 120X.

Movie S2

GFP::Ubiquitin is rapidly recruited around sperm DNA after oocyte fertilization. Every 1 second single fluorescent images were acquired for GFP (ubiquitin) and mCherry (histone) on a LSM Zeiss confocal microscope. Posterior pole is on the right. Playback: 10X.

Movie S3

CMXRos stained sperm inherited mitochondria (red) are not marked by K63- (left) nor K48- (right) linked ubiquitination (green). Confocal stacks through the sperm DNA (blue) region of a fixed meiosis II embryos. Z-stacks of images acquired every 0.4 µm. Scale bars are 1µm.

References and Notes

1. C. W. Birky Jr., The inheritance of genes in mitochondria and chloroplasts: Laws, mechanisms, and models. *Annu. Rev. Genet.* **35**, 125 (2001).

2. M. Schwartz, J. Vissing, Paternal inheritance of mitochondrial DNA. *Ugeskr. Laeger* **165**, 3627 (2003).

3. B. J. Battersby, J. C. Loredo-Osti, E. A. Shoubridge, Nuclear genetic control of mitochondrial DNA segregation. *Nat. Genet.* **33**, 183 (2003).

4. W. Y. Tsang, B. D. Lemire, Stable heteroplasmy but differential inheritance of a large mitochondrial DNA deletion in nematodes. *Biochem. Cell Biol.* **80**, 645 (2002).

5. P. Sutovsky *et al*., Ubiquitin tag for sperm mitochondria. *Nature* **402**, 371 (1999).

6. Y. Nishimura *et al*., Active digestion of sperm mitochondrial DNA in single living sperm revealed by optical tweezers. *Proc. Natl. Acad. Sci. U.S.A.* **103**, 1382 (2006).

7. T. Yoshimori, T. Noda, Toward unraveling membrane biogenesis in mammalian autophagy. *Curr. Opin. Cell Biol.* **20**, 401 (2008).

8. S. Tsukamoto *et al*., Autophagy is essential for preimplantation development of mouse embryos. *Science* **321**, 117 (2008).

9. N. L. Washington, S. Ward, FER-1 regulates Ca2+ -mediated membrane fusion during *C. elegans* spermatogenesis. *J. Cell Sci.* **119**, 2552 (2006).

10. S. Ward, Y. Argon, G. A. Nelson, Sperm morphogenesis in wild-type and fertilization-defective mutants of *Caenorhabditis elegans*. *J. Cell Biol.* **91**, 26 (1981).

11. F. Farina *et al*., Differential expression pattern of the four mitochondrial adenine nucleotide transporter ant genes and their roles during the development of *Caenorhabditis elegans*. *Dev. Dyn.* **237**, 1668 (2008).

12. Y. Tian *et al*., *C. elegans* screen identifies autophagy genes specific to multicellular organisms. *Cell* **141**, 1042 (2010).

13. A. Alberti, X. Michelet, A. Djeddi, R. Legouis, The autophagosomal protein LGG-2 acts synergistically with LGG-1 in dauer formation and longevity in *C. elegans*. *Autophagy* **6**, 622 (2010).

14. J. M. Parry *et al*., EGG-4 and EGG-5 link events of the oocyte-to-embryo transition with meiotic progression in *C. elegans*. *Curr. Biol.* **19**, 1752 (2009).

15. V. Kirkin, D. G. McEwan, I. Novak, I. Dikic, A role for ubiquitin in selective autophagy. *Mol. Cell* **34**, 259 (2009).

16. C. Kang, Y. J. You, L. Avery, Dual roles of autophagy in the survival of *Caenorhabditis elegans* during starvation. *Genes Dev.* **21**, 2161 (2007).

17. S. Jager *et al*., Role for Rab7 in maturation of late autophagic vacuoles. *J. Cell Sci.* **117**, 4837 (2004).

Supporting References

S1. S. Brenner, The genetics of *Caenorhabditis elegans*. *Genetics* **77**, 71 (1974).

S2. V. Praitis *et al*., Creation of low-copy integrated transgenic lines in *Caenorhabditis elegans*. *Genetics* **157**, 1217 (2001).

S3. R. S. Kamath *et al*., Systematic functional analysis of the *Caenorhabditis elegans* genome using RNAi. *Nature* **421**, 231 (2003).

S4. V. Galy, I. W. Mattaj, P. Askjaer, *Caenorhabditis elegans* nucleoporins Nup93 and Nup205 determine the limit of nuclear pore complex size exclusion in vivo. *Mol. Biol. Cell* **14**, 5104 (2003).

S5. K. Newton *et al*., Ubiquitin chain editing revealed by polyubiquitin linkage-specific antibodies. *Cell* **134**, 668 (2008).

S6. N. Dard, S. Louvet-Vallée, A. Santa-Maria, B. Maro, Phosphorylation of ezrin on threonine T567 plays a crucial role during compaction in the mouse early embryo. *Dev. Biol.* **271**, 87 (2004).

S7. D. J. Burke, S. Ward, Identification of a large multigene family encoding the major sperm protein of *Caenorhabditis elegans*. *J. Mol. Biol.* **171**, 1 (1983).

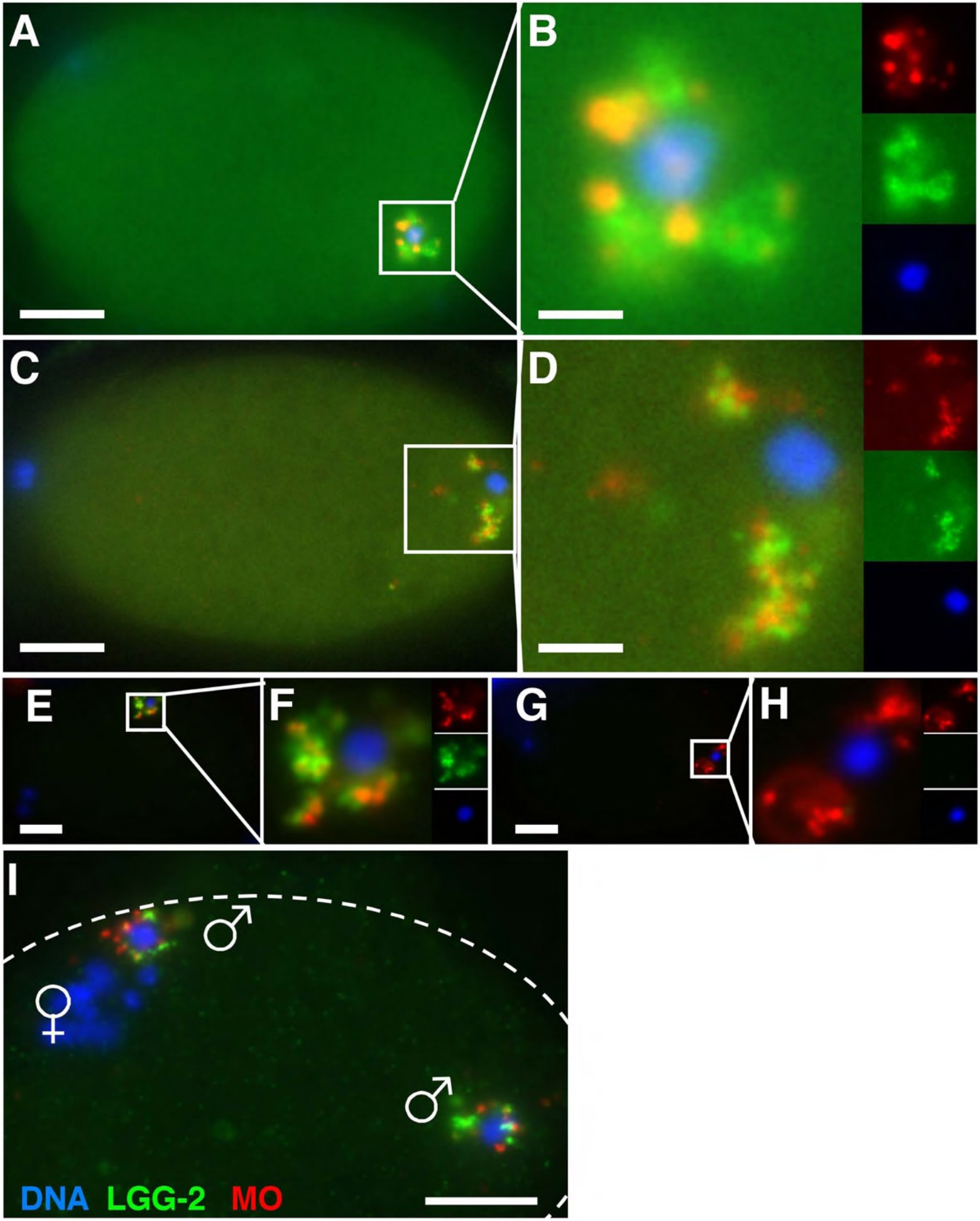
A
B
C
D
E
F
G
H
I
DNA LGG-2 MO

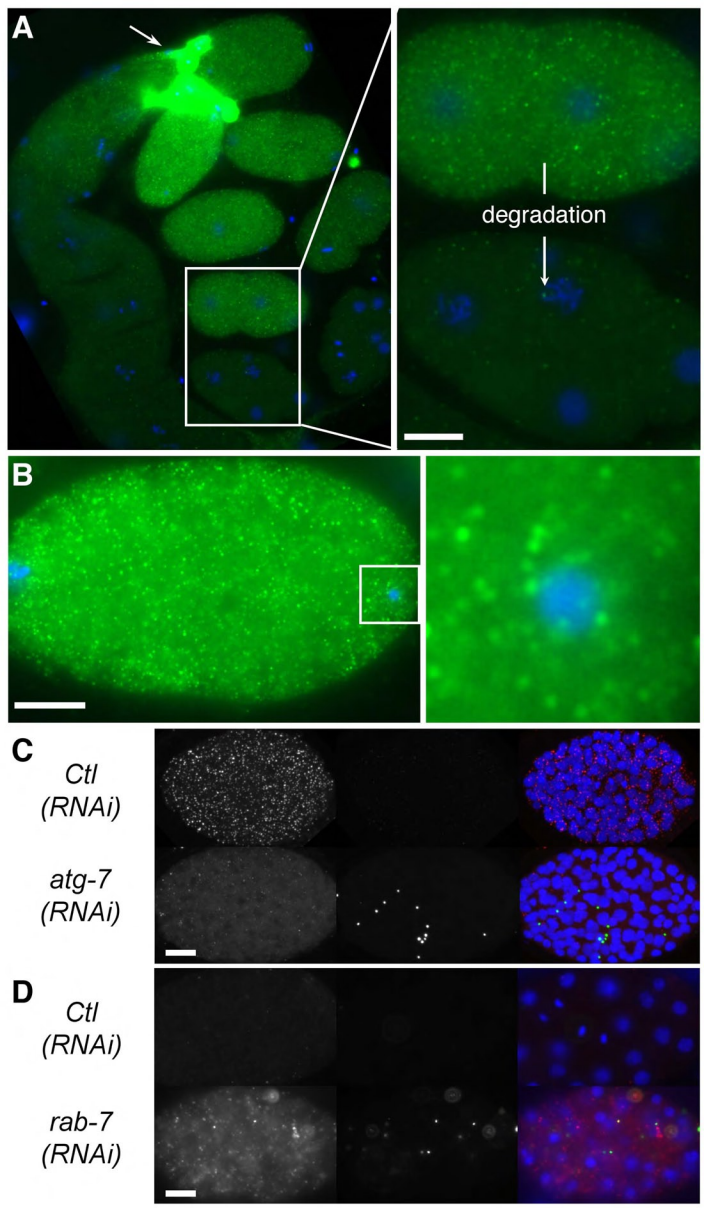
A
degradation
B
C
Ctl
(RNAi)
atg-7
(RNAi)
D
Ctl
(RNAi)
rab-7
(RNAi)

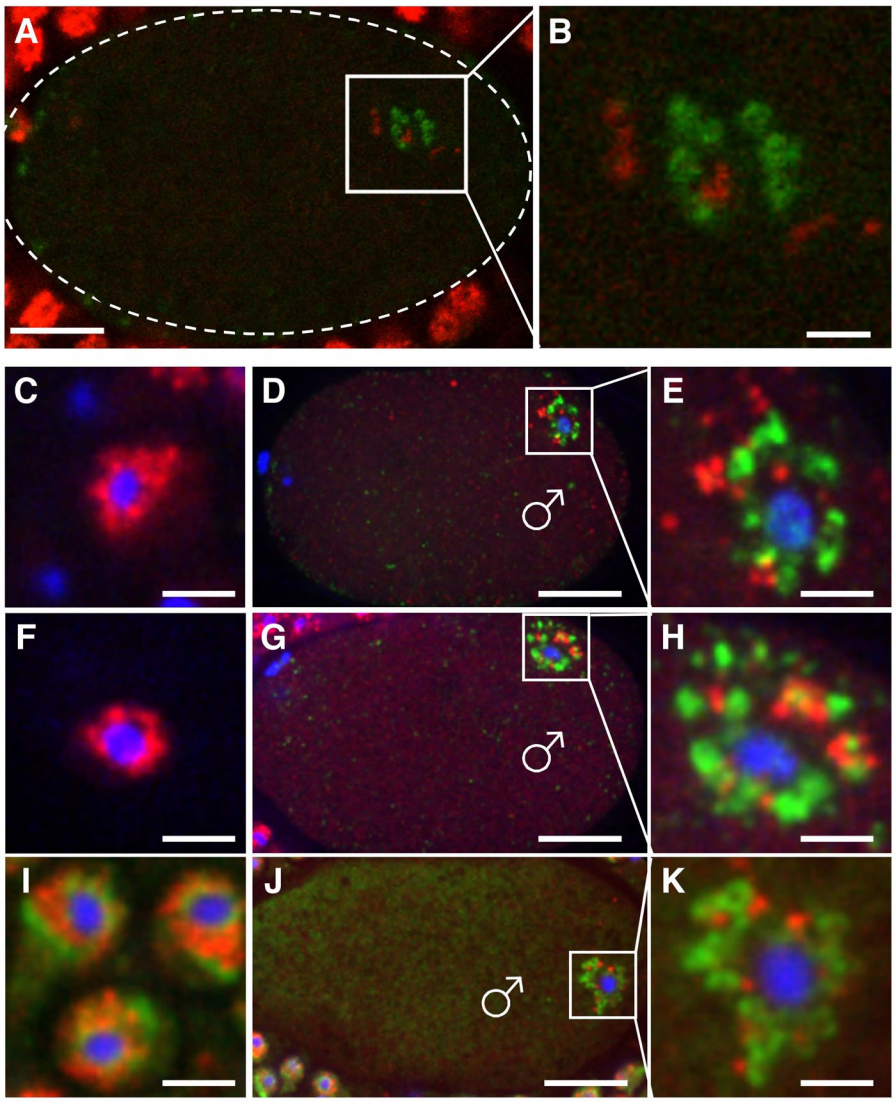
A
B
C
D
E
♂
F
G
H
♂
I
J
K
♂

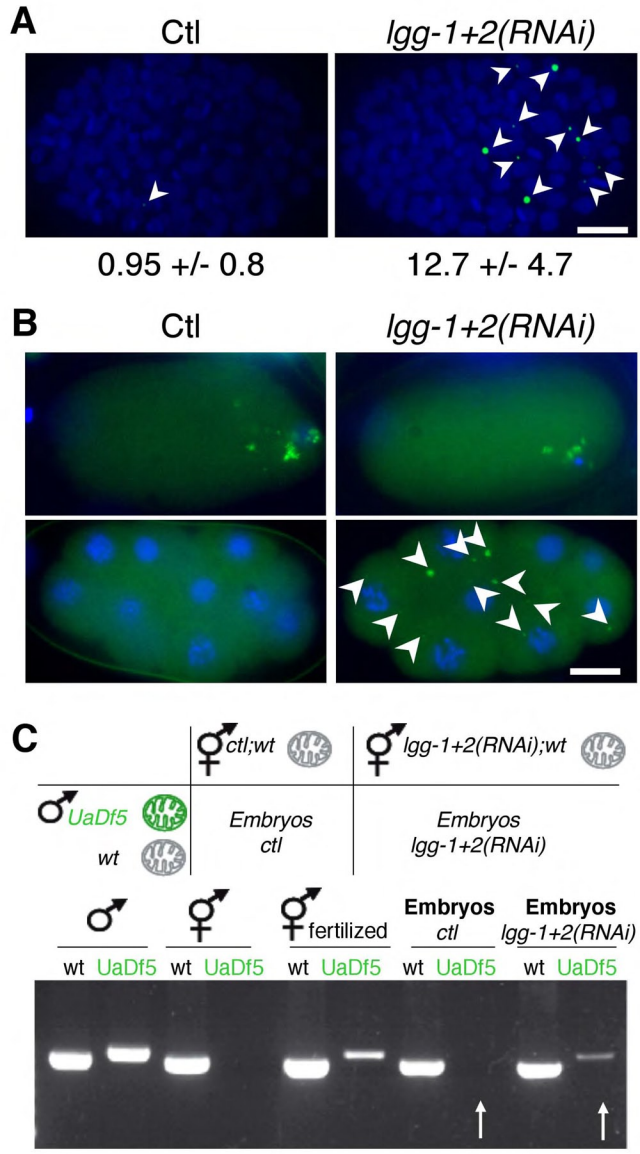
A
Ctl
lgg-1+2(RNAi)
0.95 +/- 0.8
12.7 +/- 4.7
B
Ctl
lgg-1+2(RNAi)
C
ctl;wt
lgg-1+2(RNAi);wt
UaDf5
wt
Embryos
ctl
Embryos
lgg-1+2(RNAi)
fertilized
Embryos
ctl
Embryos
lgg-1+2(RNAi)
wt UaDf5 wt UaDf5 wt UaDf5 wt UaDf5 wt UaDf5

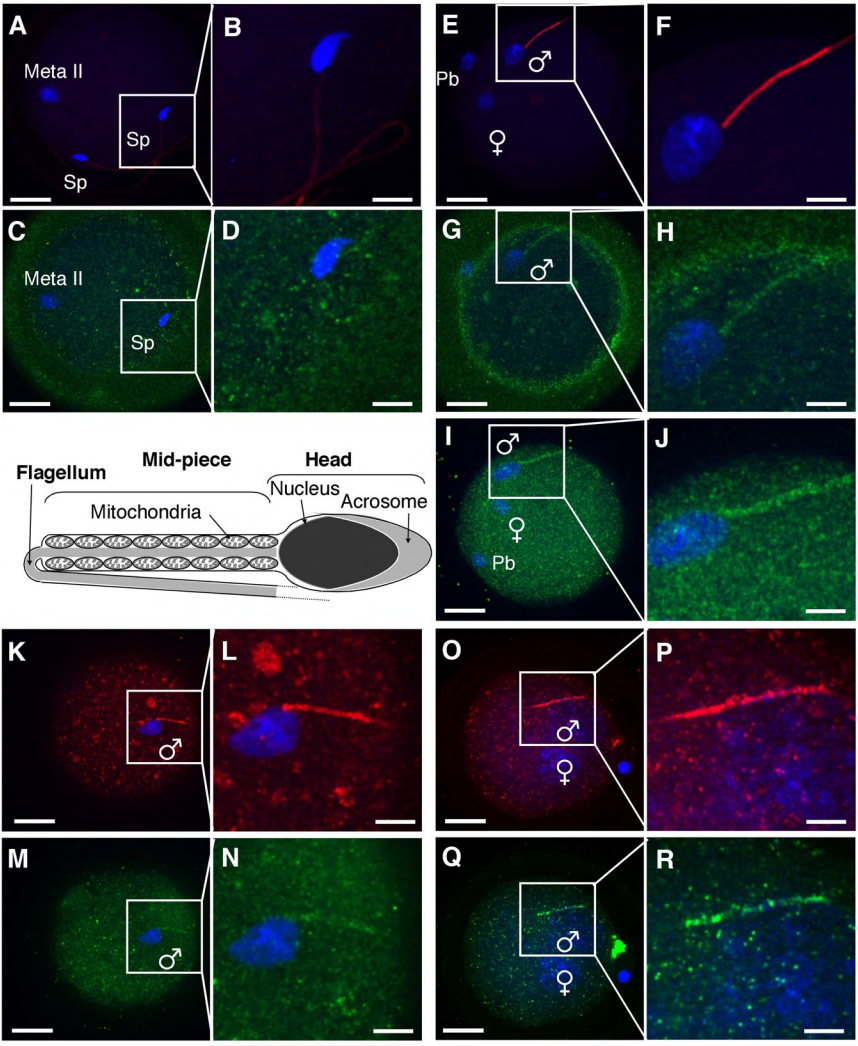
A
Meta II
Sp
Sp
B
E
Pb
♂
♀
F
C
Meta II
Sp
D
G
♂
H
Flagellum
Mid-piece
Head
Nucleus
Acrosome
Mitochondria
I
♂
♀
Pb
J
K
♂
L
O
♂
♀
P
M
♂
N
Q
♂
♀
R